Distinct structural and mechanical properties of the nuclear lamina in Hutchinson–Gilford progeria syndrome

Kris Noel Dahl*†‡§, Paola Scaffidi†¶, Mohammad F. Islam‖**, Arjun G. Yodh‖, Katherine L. Wilson*, and Tom Misteli¶

*Department of Cell Biology, Johns Hopkins University School of Medicine, Baltimore, MD 21205; ¶National Cancer Institute, National Institutes of Health, Bethesda, MD 20892; and ‖Department of Physics and Astronomy, University of Pennsylvania, Philadelphia, PA 19104

Edited by Mark T. Groudine, Fred Hutchinson Cancer Research Center, Seattle, WA, and approved May 26, 2006 (received for review March 3, 2006)

The nuclear lamina is a network of structural filaments, the A and B type lamins, located at the nuclear envelope and throughout the nucleus. Lamin filaments provide the nucleus with mechanical stability and support many basic activities, including gene regulation. Mutations in *LMNA*, the gene encoding A type lamins, cause numerous human diseases, including the segmental premature aging disease Hutchinson–Gilford progeria syndrome (HGPS). Here we show that structural and mechanical properties of the lamina are altered in HGPS cells. We demonstrate by live-cell imaging and biochemical analysis that lamins A and C become trapped at the nuclear periphery in HGPS patient cells. Using micropipette aspiration, we show that the lamina in HGPS cells has a significantly reduced ability to rearrange under mechanical stress. Based on polarization microscopy results, we suggest that the lamins are disordered in the healthy nuclei, whereas the lamins in HGPS nuclei form orientationally ordered microdomains. The reduced deformability of the HGPS nuclear lamina possibly could be due to the inability of these orientationally ordered microdomains to dissipate mechanical stress. Surprisingly, intact HGPS cells exhibited a degree of resistance to acute mechanical stress similar to that of cells from healthy individuals. Thus, in contrast to the nuclear fragility seen in *lmna* null cells, the lamina network in HGPS cells has unique mechanical properties that might contribute to disease phenotypes by affecting responses to mechanical force and misregulation of mechanosensitive gene expression.

laminopathy | mechanics | nucleus | photobleaching | micropipette aspiration

Hutchinson–Gilford progeria syndrome (HGPS) is a rare genetic disease that causes segmental premature aging in children. HGPS patients are mentally normal, but fail to reach full stature and experience hair loss, thin wrinkled skin, and joint stiffness, and usually die in their early teens of cardiovascular disease or stroke (1, 2). Mutations in *LMNA*, the gene encoding lamins A and C, were recently identified as the cause of HGPS (3, 4). Lamins A and C are major constituents of the nuclear lamina, the meshwork of nuclear intermediate filaments that support the inner nuclear membrane and also extend throughout the nucleus (5). Other major components of the nuclear lamina are lamins B1 and B2, which are encoded by two distinct genes (6). Most HGPS cases are caused by a *de novo* single-point mutation (G608G; GGC>GGT) in one allele of *LMNA* (3, 4). This substitution activates a cryptic splice site in exon 11, which affects only the lamin A protein, and the mutant allele produces an alternatively spliced truncated variant of the lamin A mRNA lacking the 3′ terminal 150 nt of exon 11. The resulting polypeptide, Δ50 lamin A, has an internal deletion of 50 residues in the C-terminal tail domain and also lacks an endoproteolytic cleavage site required for normal processing of the lamin A precursor (3, 4, 7). HGPS patient fibroblasts often are characterized by numerous nuclear defects, including abnormal morphology, altered histone modification patterns, and increased DNA damage (8–10).

Lamins are directly implicated in the structural integrity of the nucleus. Nuclei assembled in lamin-depleted *Xenopus* egg extracts are highly fragile (11), and nuclei from mouse *lmna* null cells are mechanically weak (12). *In vitro* rheology of reconstituted lamin B1 solutions shows lamin filaments to be stiff but elastic, with resilience under shear deformation (13). Direct mechanical measurements of *Xenopus* oocyte nuclei further reveal the *in vivo* lamina to be a stiff network, which is reversibly expandable (14).

Mutations in *LMNA* cause multiple human diseases other than HGPS. Notably, tissues affected by various "laminopathies" are under considerable mechanical stress (15), suggesting mechanical weakness of the lamina might contribute directly or indirectly to disease phenotypes. Alternative models suggest defective tissue-specific gene expression (15, 16). These models are not mutually exclusive, because cells that lack A type lamins have mechanotransduction defects that lead to misregulation of mechanosensitive genes (12, 17).

One of the classic hallmarks of HGPS nuclei are dramatic changes in nuclear morphology (3, 4, 8). It, however, has not yet been demonstrated that the mechanical properties of the lamina are altered in HGPS patient cells. Here we have determined the effect of the HGPS mutation on the dynamics, structure, and mechanical properties of the lamina.

Results

Dynamic Properties of Lamins in HGPS Cells. We first sought to quantitatively compare the dynamics of lamins in WT and HGPS cells. To this end, we performed fluorescence recovery after photobleaching assays. In agreement with previous studies (8, 9), in WT cells, GFP-lamin A showed a strong biphasic recovery after photobleaching; ≈15% of the fluorescent signal recovered rapidly within 15 s after photobleaching, whereas the remaining ≈85% showed slow but steady recovery (Fig. 1 *A* and *B*). This behavior is indicative of two kinetically distinct populations of lamin A, with one fraction dynamically exchanging between the lamina and the nucleoplasm and a second more stable population. In contrast, the entire population of GFP-fused Δ50 lamin A was nearly immobile, indicating that Δ50 lamin A associates irreversibly with the lamina (Fig. 1 *A* and *B*). This observation is consistent with the increased lamina thickness seen by light and electron microscopy (8). When WT GFP-lamin A was expressed in HGPS cells, on the other hand, it became partially immobilized with <5% of the signal recovered 15 s after

Conflict of interest statement: No conflicts declared.

This paper was submitted directly (Track II) to the PNAS office.

Abbreviations: HGPS, Hutchinson–Gilford progeria syndrome; MPA, micropipette aspiration.

†K.N.D. and P.S. contributed equally to this work.

‡Present address: Departments of Biomedical Engineering and Chemical Engineering, Carnegie Mellon University, Pittsburgh, PA 15213.

§To whom correspondence should be addressed. E-mail: krisdahl@cmu.edu.

**Present address: Departments of Chemical Engineering and Materials Science and Engineering, Carnegie Mellon University, Pittsburgh, PA 15213.

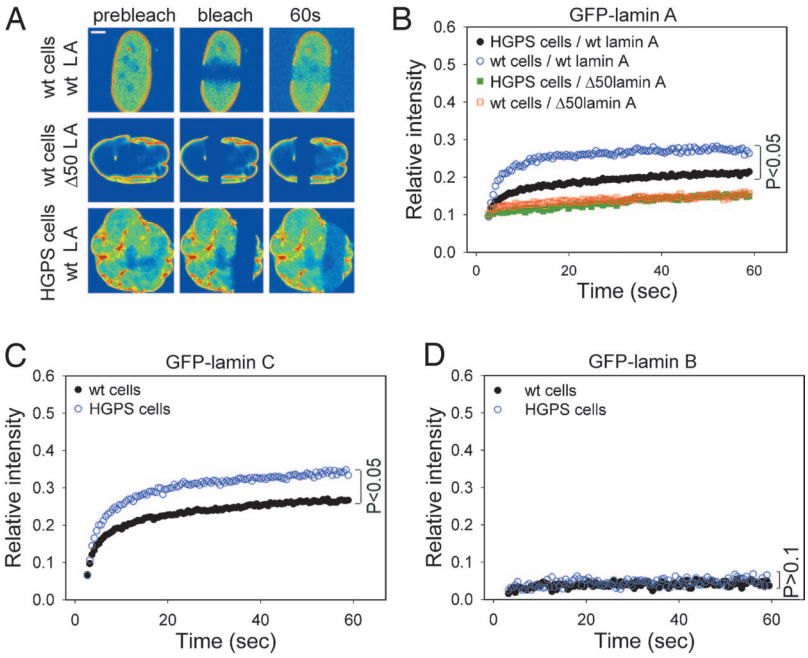

Fig. 1. Reduced dynamic exchange of A type lamins in HGPS cells. (*A*) WT and HGPS cells expressing either WT or Δ50 GFP-lamin A were imaged before and during recovery after bleaching of a part of the nucleus. Images are shown by using intensity pseudocolors. Contrast was adjusted in the 60-s frame to visually normalize for total loss of fluorescence during imaging. (Scale bar: 5 μm.) (*B–D*) Quantitative analysis of fluorescence recovery after photobleaching recovery in WT and HGPS cells. Kinetics of recovery of the fluorescence signal in the whole bleached area in cells expressing either WT or Δ50 GFP-lamin A (*B*), WT lamin C (*C*), or WT lamin B (*D*). The statistical significance of the difference between the two recovery curves is indicated. Values represent means from at least 10 cells each from three experiments. Standard errors were between 10% and 20%.

photobleaching (Fig. 1 *A* and *B*). This behavior is consistent with a dominant mode of action of Δ50 lamin A (9). As a control, the entire population of GFP-fused Δ50 lamin A was immobile in HGPS cells (Fig. 1*B*).

We also measured the exchange dynamics of GFP-fused lamins C and B1 in HGPS cells. In WT cells, GFP-lamin C recovered biphasically with a small rapidly exchanging fraction and a large slowly exchanging fraction (Fig. 1*C*, open circles). As observed for GFP-lamin A, the rapidly exchanging fraction of GFP-lamin C was reduced significantly in HGPS cells (Fig. 1*C*, closed circles; $P < 0.05$), suggesting all endogenous A type lamins become relatively immobile in HGPS cells. In contrast, as a control, GFP-lamin B1 was virtually immobile in WT cells and no significant recovery was detected over 60 s (Fig. 1*D*; $P > 0.1$). We concluded that lamin B1 associates more stably with the lamina network than A type lamins and does not exchange detectably after integration. The recovery kinetics of GFP-lamin B1 were not detectably different in HGPS cells (Fig. 1*D*).

To independently confirm the reduced lamin dynamics in HGPS cells, we performed biochemical extractions. Nuclei isolated from HeLa cells expressing either WT or Δ50 GFP-lamin A were sequentially extracted with increasing concentrations of salt, and the supernatants and insoluble pellets were analyzed by Western blotting with the anti-GFP antibody (Fig. 2*A*). Approximately 10% of WT GFP-lamin A was extracted by 250 mM NaCl, and an additional ≈20% was released at 500 mM NaCl. In contrast, no detectable Δ50 GFP-lamin A was extracted by 250 mM NaCl, and only trace amounts were released at 500 mM (Fig. 2*A*). This result confirmed that Δ50 GFP-lamin A associates more tightly with the nuclear lamina than WT GFP-lamin A.

To test whether Δ50 lamin A affected the solubility of endogenous lamins as expected based on the fluorescence recovery after photobleaching results, the same blots were probed with an antibody against lamins A and C. In control cells expressing WT GFP-lamin A, small amounts of endogenous lamins A and C were extracted by 250 mM salt, and ≈20% of each was extracted by 500 mM NaCl (Fig. 2*A Lower*). In contrast, nuclei from cells expressing Δ50 GFP-lamin A released <5% of endogenous lamins A and C after extraction by 500 mM NaCl (Fig. 2*A*). We conclude that even small amounts of Δ50 lamin A are sufficient to immobilize endogenous WT A type lamins in the lamina network.

We also salt-extracted lamins from HGPS versus control fibroblasts. In control cells, <5% of lamin A and C were released by 250 mM NaCl and ≈10% at 500 mM NaCl (Fig. 2*B*). In HGPS cells, which express similar levels of each A type lamin, only ≈5% of WT lamins A and C and trace amounts of Δ50 lamin A were extracted at 500 mM NaCl. Collectively these results indicated that the self-association of A type lamins is altered in HGPS cells.

Salt-Induced Dilation and Recovery of Isolated Nuclei. Given the abnormally stable interactions of A type lamins in HGPS cells,

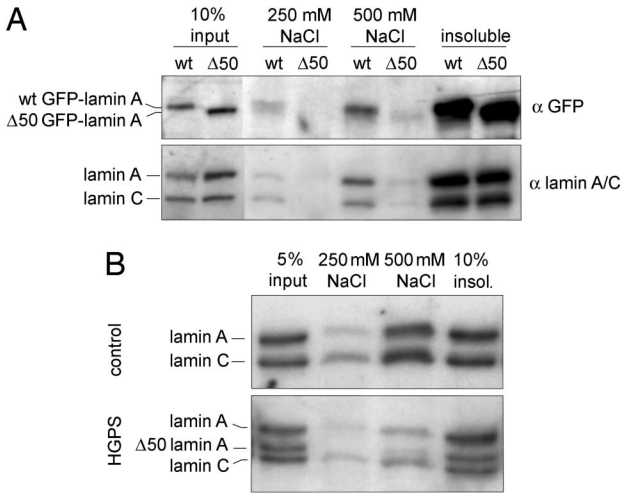

Fig. 2. Reduced extractability of A type lamins in HGPS cells. (*A*) Western blot analysis of isolated nuclei from HeLa cells expressing either WT or Δ50 GFP-lamin A after extraction with increasing concentrations of NaCl. The samples were probed with anti-GFP and anti-lamin A/C antibody. Δ50 GFP-lamin A is less extractable than the WT protein and reduces the extractability of endogenous WT lamin A and lamin C. (*B*) Western blot analysis of isolated nuclei from control and HGPS fibroblasts after extraction with increasing concentrations of NaCl. Endogenous Δ50 lamin A is less extractable than WT protein in HGPS. Also the extractability of WT lamin A and lamin C is reduced in HGPS versus WT cells.

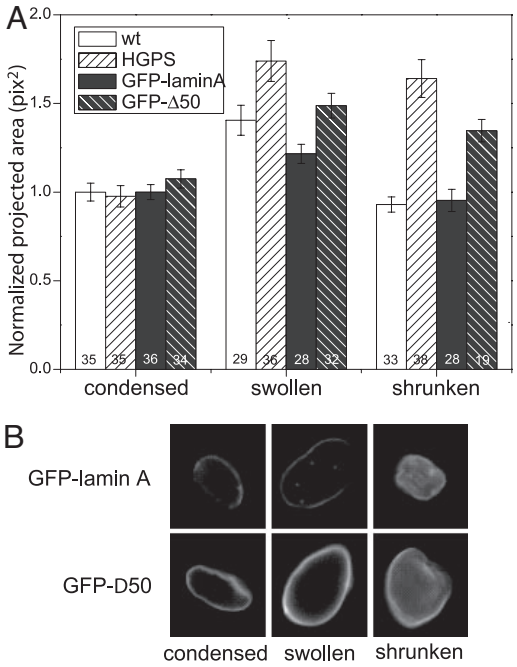

Fig. 3. Swelling and shrinking behavior of isolated nuclei. (*A*) Quantitative analysis of swelling and shrinking. The projected area of nuclei was calculated and normalized. All fibroblast data (WT and HGPS) was normalized such that the condensed WT nucleus average was 1. All HeLa data (GFP-lamin A or GFP-Δ50) was normalized such that the condensed GFP-lamin A nuclear average was 1. Swollen HGPS or Δ50 GFP-lamin A nuclei were slightly larger than their respective control nuclei (Student *t* test; $P = 0.023$, HGPS; $P = 0.003$, Δ50 GFP-lamin A). Differences between shrunken control and HGPS or Δ50 lamin A transfected nuclei were all significant at $P < 0.001$ in a Student *t* test. Numbers of measured nuclei for each condition are indicated. Graphed values represent averages ± SEM of the projected area. (*B*) Differential behavior seen in nuclei isolated from HeLa cells transfected with GFP-lamin A or Δ50 GFP-lamin A in their condensed (high divalent salt), swollen (near-zero salt) and shrunken (swollen with added divalent salt) states.

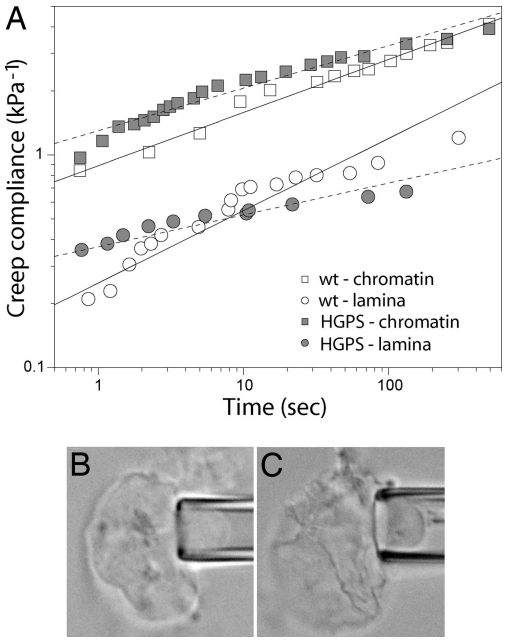

Fig. 4. MPA of isolated nuclei. (*A*) The creep compliance, a function of the increased deformation into the micropipette at a step pressure, is plotted versus time. Data points from one experiment are overlaid with lines, which are fits of the combined data (a modified form of this data are in Table 1). HGPS and WT nuclei show no difference in chromatin mechanics on this measurement length scale. The slope of the creep compliance for the lamina-dominated measurement is higher in WT than HGPS nuclei, indicating that WT deforms more easily over time. (*B* and *C*) Control nuclei buckled relatively smoothly outside the pipette as aspiration increased (*B*), indicating that mechanical stresses were distributed across the entire lamina. In striking contrast, the lamina of HGPS nuclei collapsed along long prominent fault lines, appearing crumpled or folded (*C*).

we hypothesized that the biophysical properties of the HGPS lamina might be affected. We measured the ability of isolated nuclei to reversibly dilate and condense in response to changes in salt concentration, a simple quantitative measure of the lamina's ability to rearrange (18). Under high divalent salt (3 mM $MgCl_2$/3 mM $CaCl_2$; see *Methods*) conditions, the condensed WT and HGPS nuclei were similar in size as assessed by their 2D projected nuclear area (Fig. 3*A*, condensed). In near-zero salt conditions, HGPS nuclei appeared slightly larger than controls (Fig. 3*A*, swollen; $P = 0.023$). However, when nuclei were treated with concentrated salts to reverse the swelling, significant differential behavior was observed between WT and HGPS cells (Fig. 3). WT nuclei reproducibly shrank back to their original size in <5 min (Fig. 3*A*), as expected (18). In striking contrast, HGPS nuclei did not resume their original condensed size even after 20–30 min (Fig. 3, compare swollen to shrunken HGPS; $P = 0.53$). To directly confirm that these differences were due to the presence of Δ50 lamin A protein and not secondary effects in HGPS cells, we repeated these experiments in HeLa cells transfected with either GFP-lamin A as a control or with Δ50 GFP-lamin A (Fig. 3). Similar to HGPS cells, the mutant lamin A protein had little effect on the swelling of the nuclei but subsequently prevented shrinkage (Fig. 3, compare swollen to shrunken GFP-Δ50; $P = 0.14$). We concluded that the HGPS nuclear lamina can dilate near-normally but is impaired in its ability to condense and reorganize back into a smaller space. We further conclude that the inability to condense is due solely to the mutant lamin A protein, because exogenous expression in HeLa cells produced the same phenotype.

Micropipette Aspiration of Isolated Nuclei from HGPS Cells. To better quantify the mechanical properties of HGPS nuclei, we used micropipette aspiration (MPA). In this method, isolated nuclei are aspirated at constant pressure with a glass micropipette, and their deformation is measured as a function of time (see *Supporting Methods*, which is published as supporting information on the PNAS web site, and ref. 18). The creep compliance, defined as the deformability of the nucleus at a step stress, can be calculated from MPA data and is a measure of a material's viscoelastic deformability. For isolated nuclei in which chromatin is condensed, the MPA method reveals primarily the mechanical properties of chromatin. By contrast, in swollen nuclei with decondensed chromatin, MPA probes the mechanical properties of the nuclear lamina (18).

Nuclei isolated from either WT or HGPS cells directly into divalent salts (condensed, chromatin-dominated state) responded similarly to aspiration pressure (Fig. 4*A*, open and filled squares), suggesting that gross mechanical differences in chromatin organization in HGPS nuclei on this measurement length scale do not exist. In contrast, when we tested the properties of the lamina itself by aspirating decondensed nuclei, we detected significant differences between WT and HGPS nuclei. Specifically the slope of the creep compliance was higher in WT nuclei than HGPS (Fig. 4*A*, filled versus open circles), indicating that the WT lamina has a greater ability to deform over time.

The above mechanical measurements were based only on the section of the nucleus inside the pipette (18, 19). Examination of

CELL BIOLOGY

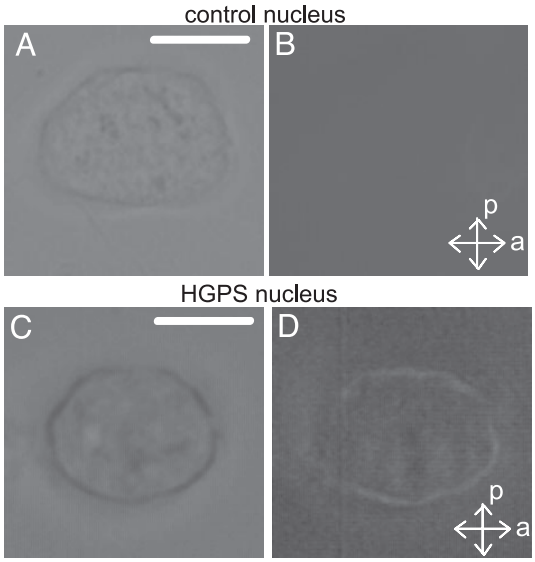

Fig. 5. Polarized light microscopy. (*A* and *B*) Isolated WT nuclei (shown in brightfield in *A*) showed no detectable birefringence (*B*) at any angle, suggesting completely isotropic orientation of lamin filaments. (*C* and *D*) As isolated HGPS nuclei (brightfield; *C*) were rotated with respect to the crossed polarizers, a bright birefringent pattern was detected at the nuclear periphery possibly due to filament alignment (*D*). (Scale bars: 4 μm.)

those parts of the nucleus outside the pipette revealed, in addition, a unique force distribution pattern in HGPS nuclei (Fig. 4 *B* and *C*). Specifically, WT nuclei buckled relatively smoothly outside the pipette as aspiration increased (Fig. 4*B*), indicating that mechanical stresses were distributed across the entire peripheral lamina. In striking contrast, the lamina of HGPS nuclei collapsed along long prominent fault lines, appearing crumpled or folded (Fig. 4*C*), similar to the "wrinkles" characteristic of HGPS nuclei (8). The combination of these observations points to distinct mechanical properties of the lamina of HGPS cells.

HGPS Lamina Is Birefringent, Consistent with an Orientationally Ordered Lamina. Structural failure along major fault lines in HGPS cells might be caused by differences in the microorganization of lamin filaments in the lamina network. To test this hypothesis, we used polarization light microscopy. Isotropic regions (random orientation) and regions where the lamins align along the polarizer axis should appear dark in polarization microscopy, and regions in which the lamins align at 45° to the polarizer axes should appear bright (20). None of the >20 isolated WT nuclei examined (shown in brightfield in Fig. 5*A*) exhibited detectable birefringence at any angle (Fig. 5*B*). This observation suggests that the orientation of the lamin filaments in the WT lamina is isotropic. In contrast, the periphery of all of the >20 isolated HGPS nuclei examined (brightfield; Fig. 5*C*) appeared birefringent when viewed between crossed polarizers (Fig. 5*D*). This observation suggests that lamin filaments in the nuclear periphery could be aligned (see *Supporting Methods*). We did not notice any change in the birefringent intensity when the HGPS nucleus was rotated between the crossed polarizers, suggesting that the lamin filaments have assembled into many small, uncorrelated, but orientationally ordered microdomains, each large enough to exhibit birefringence (see *Supporting Methods*).

Nuclear Stability in Intact HGPS Cells. Because our mechanical measurements suggest that HGPS nuclear lamina is less able to rearrange after stress compared with WT nuclei, we probed the mechanical resistance of the nucleus in intact cells challenged by

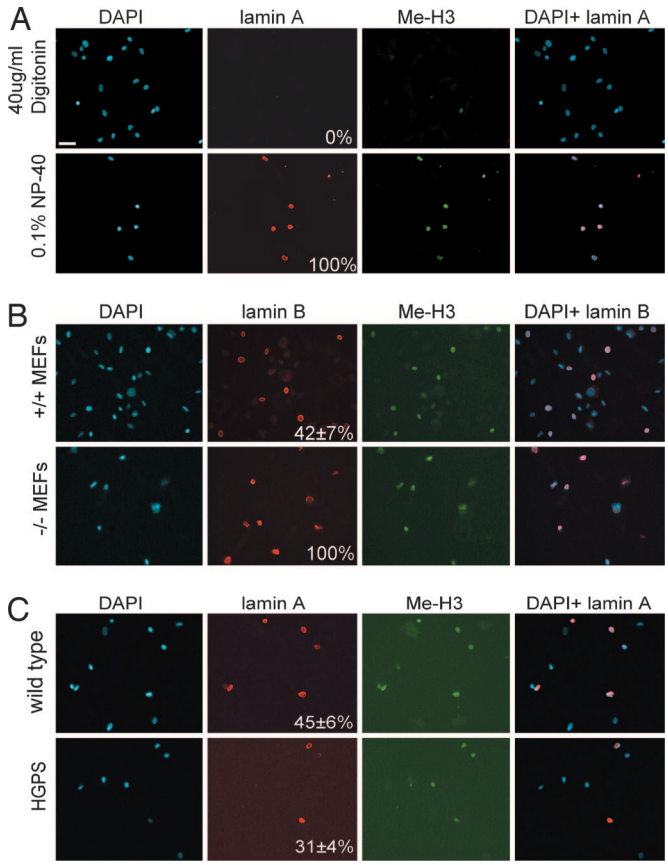

Fig. 6. *In vivo* pressure assay. Immunofluorescence microscopy of WT (*A* and *C*) and HGPS (*C*) primary dermal fibroblasts and *lmna* $^{/}$ and *lmna* $^{-/-}$ MEFs (*B*) after exposure to 700-kPa pressure. Cells were stained with DAPI and antibodies against the indicated proteins in the absence of detergents. (Scale bar: 80 μm.) The percentage of staining-positive cells is indicated. $n \geq 300$ per condition.

pressure. Cells were incubated under hypoosmotic conditions to swell and then were exposed to 700 kPa physical pressure (see *Methods*). The integrity of the nuclear envelope was assayed after fixation by the accessibility of antibodies against nuclear epitopes, including lamin A and tri-meK4H3 in the absence of detergents (Fig. 6; see also Fig. 8, which is published as supporting information on the PNAS web site). To validate that antibody accessibility indeed reported nuclear rupture, WT cells were incubated with 40 μg/ml digitonin to selectively permeabilize the plasma membrane, but not nuclear membranes, or with 0.1% Nonidet P-40 to permeabilize both the plasma membrane and nuclear envelope (Fig. 6*A*). As expected, antibodies did not enter the nucleus of digitonin-treated control cells but did enter control cells permeabilized by Nonidet P-40 (Fig. 6*A*). As a positive control, we compared mouse embryonic fibroblasts (MEFs) from WT or *lmna*$^{-/-}$ mice, which have impaired mechanical resistance (12). Under our experimental conditions, 100% of *lmna*$^{-/-}$ MEF nuclear envelopes became accessible to antibodies, whereas only 42 ± 7% of WT nuclei did under the same conditions (Fig. 6*B*). Interestingly, the HGPS patient cells were slightly more resistant to nuclear envelope rupture than WT fibroblasts: 31 ± 4% of HGPS nuclei ruptured compared with 45 ± 6% of WT nuclei (Fig. 6*C*). These results suggest that the altered mechanical properties of the lamina in HGPS cells do not increase nuclear fragility in response to gross mechanical force; if anything, HGPS nuclei appear more resistant to mechanical stress.

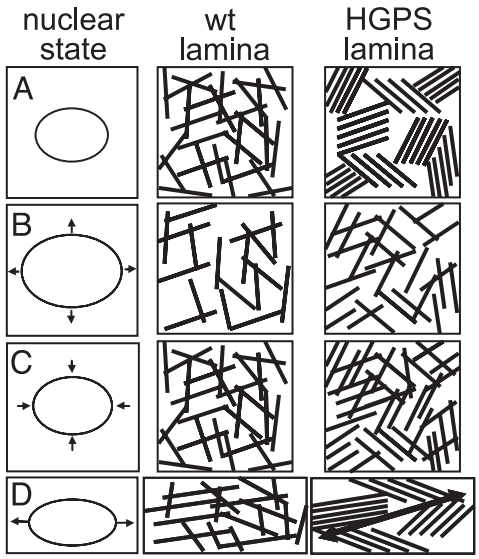

Fig. 7. Model of HGPS nuclear lamina ultrastructure and responses to force. Isotropic filaments in WT nuclei can expand reversibly and easily (*A–C*, wt lamina). However, the order in the HGPS lamina (*A*, HGPS lamina) is lost when surface area increases, because lamins can occupy a larger space (*B*, HGPS lamina). Upon sudden compression, there is insufficient time to return to the ordered state, and the lamina forms a jammed state (*C*, HGPS lamina). Isotropic filaments can realign easily along any director of force and redistribute the force evenly (*D*, wt lamina). Microdomains tend to move as whole domains and align their preferred orientation to be parallel with the director of the force (*D*, HGPS lamina).

Discussion

We have compared the structural and mechanical properties of HGPS and normal fibroblast nuclei. We find significant alterations in the mechanical properties and organization of the HGPS lamina. The lamins in HGPS cells resisted biochemical extraction, had significantly reduced rates of exchange with the soluble pool of lamins *in vivo*, and the lamina was birefringent. Importantly, the HGPS nuclear lamina expanded normally in response to dilation forces but was unable to return to normal after stretching. This change also was seen in HeLa cells with exogenously expressed Δ50-lamin A protein, demonstrating that the observed mechanical properties are directly due to the presence of the mutant lamin A protein. Remarkably, these changes to the lamina did not make HGPS nuclei more fragile when intact cells were subjected to mechanical force.

An important clue regarding the HGPS molecular defects came from our observation that the HGPS lamina is birefringent, possibly due to lamin alignment. We hypothesize that the lamins form ordered microdomains by closely packing near the inner nuclear membrane; in this case, orientationally ordered (nematic) domains would result as molecules try to fit into confined spaces (see *Supporting Methods*). Indeed, at high concentration, lamins form paracrystals *in vitro* (21). Our model that HGPS lamins form locally ordered, nematic microdomains is supported by the fault lines seen during aspiration (Fig. 7), because microdomains would respond to stress by aligning along the direction of the applied force (22). Ordered microdomains also can explain our MPA results and our finding that HGPS nuclei could expand but subsequently failed to return to their original size (Fig. 7). With even more time, increased lamin accumulation could cause the lamina to rupture as seen with the lobed nuclei discussed elsewhere (8, 9).

Surprisingly, the changes in the HGPS lamina did not appear to compromise the overall mechanical resistance of nuclei to pressure *in vivo*. In fact, whole HGPS nuclei were, if anything, slightly more resistant to mechanical pressure than normal nuclei. One major function of the lamina is to resist deformation of the nucleus (23). In intact tissues, the nucleus and nuclear envelope are constantly exposed to high levels of mechanical stress, particularly in tissues such as bone, skeletal muscle, heart, and blood vessels. Correspondingly, ''mechanical weakness'' models suggested that human laminopathies might be caused by nuclear fragility in cells with mutations in *LMNA*, as seen in *lmna* null mouse cells (12, 24). It is noteworthy that nuclear fragility in Emery-Dreifuss muscular dystrophy correlates with looser association of lamin A to the lamina (25), in contrast to the tighter binding observed in HGPS cells. Thus, the distinct mechanical properties of the lamina in HGPS cells demonstrate that not all mutations in *LMNA* have the same consequences, nor do they all cause mechanical fragility.

We hypothesize that the HGPS mutation has a major effect on how forces are transduced into the nucleus. We suggest that defects would impair tissue-appropriate mechanotransduction in, for example, endothelial and smooth muscle cells and, thereby, contribute to vascular defects seen in HGPS patients and model mice (26). The endothelium is exposed to different flow patterns and the vascular wall continuously fine tunes its activities in response to vascular shear stress (27). As a thought experiment using our data from Table 1, which is published as supporting information on the PNAS web site, the lamina of WT and HGPS nuclei would have the same stiffness after 30 seconds of applied force. However, after 5 min of applied force, the HGPS lamina is 4-fold less deformable. This inability to rearrange correctly may affect both mechanotransduction and the overall structure of the cell (e.g., thickness).

Finally, altered mechanical properties of the lamina in HGPS cells might lead to misexpression of mechanosensitive genes. Mechanical forces can be signaled either through biochemical signals that modulate gene expression and cell function or by direct mechanical links between the cytoskeleton and lamina (28). How cells sense external forces and respond by changes in gene expression are open questions, but both lamin A and the lamin-binding protein emerin are implicated in this process (12, 29). Changes in lamina architecture in HGPS nuclei have been shown to alter epigenetic modifications, resulting in loss of heterochromatin (9). Our findings suggest a gross reorganization of the lamina architecture into ordered domains. We conclude from these considerations that although the mechanical properties of the lamina are altered in HGPS cells, these changes do not lead to disease symptoms via increased nuclear fragility. It seems more likely that they affect nuclear function by altering mechanotransduction or the activity of mechanosensitive genes through currently unknown mechanisms.

Materials and Methods

Cell Culture and Transfection. Primary dermal fibroblast cell lines from patients and a healthy donor were obtained from the Aging Repository of the Coriell Cell Repository. HGPS cell lines were from patients of different age: samples AG01972 (14 years), AG06917 (3 years), AG11498 (14 years), and AG11513 (8 years). The WT cell line (AG08469) was from the father of a patient (38 years). Details of cell culture and transfection can be found in *Supporting Methods*.

Plasmids. The pEGFP-lamin A encoding the WT fusion protein was kindly provided by Jos Broers (Technical University of Eindoven, The Netherlands) (30). To introduce the 150-nt deletion in lamin A cDNA and generate pEGFP-Δ50, pEGFP-lamin A was used as a template in a two-step PCR mutagenesis as described in *Supporting Methods*. pEGFP-lamin C has been described in ref. 9. pEGFP-lamin B1 was kindly provided by Jan Ellenberg (European Molecular Biology Laboratory, Heidelberg, Germany) (31).

***In Vivo* Microscopy and Fluorescence Recovery After Photobleaching.** Eighteen hours after transfection, cells grown on Nalge Lab-Tek II chambers were analyzed with a Zeiss LSM 510 confocal microscope by using a 100 objective, zoom 4. Stacks of images (512 512 pixels) were recorded at maximum speed (one image every 490 msec), and recovery of fluorescence was measured as described in ref. 32. The values of fluorescence intensity were normalized singly to the initial fluorescence. Typically, ≈30% of the initial fluorescence was lost during the bleach pulse. All experiments were done at 37°C. All quantitative values represent averages from at least 10 cells each from three independent experiments.

Salt Extraction of Primary Fibroblasts and HeLa Cells. HGPS, WT fibroblasts, or HeLa cells expressing WT or Δ50 GFP-lamin A were permeabilized with 40 μg/ml digitonin in ice-cold buffer N (10 mM Tris, pH 7.4/2 mM $MgCl_2$/protease inhibitors mixture; Calbiochem). Nuclei were then extracted sequentially with ice-cold buffer E (buffer N supplemented with 0.1% Triton X-100) and buffer E supplemented with 50, 150, 250, or 500 mM NaCl. After each extraction step, the soluble material was separated from insoluble material by centrifugation at 700 *g* for 5 min at 4°C. The final insoluble pellet was resuspended in 1 Laemmli buffer and boiled for 5 min. The samples were load on 7.5% Tris-glycine mini gels along with 5% of the starting material (input) and analyzed by Western blot (see *Supporting Methods*). To estimate the percentage of lamins extracted in each fraction, the intensity of the corresponding bands was quantified by using FLUORCHEM (Alpha Innotech Corp., San Leandro, CA) software.

Nuclear Isolation and Swelling Assay. HGPS (AG01972), WT fibroblast, and HeLa nuclei were isolated from 90% confluent cultures as described in ref. 18. Nuclei were resuspended in TKMC (50 mM Tris, pH 7.6/25 mM KCl/3 mM $MgCl_2$/3 mM $CaCl_2$) for DNA-condensed state or 10 mM Tris pH 7.6 for swollen state. To "shrink" nuclei, swollen nuclei were incubated 20 min with 0.2 volumes of 5 TKMC. Sizes were measured by fluorescence microscopy (*Supporting Methods*) and as described in ref. 18.

MPA. MPA was performed as described ref. 18 and as summarized in detail in *Supporting Methods*. Pipettes of radii 2–5 μm and pressures ranging from 2.9 kPa to 16.5 kPa were used.

Polarization Microscopy. MatTek dishes (MatTek, Ashland, MA), Petri dishes with coverslips attached to holes in the bottom, were coated with polyL-lysine (Sigma-Aldrich) per manufacturer instructions. Isolated nuclei were attached to polyL-lysine nonspecifically for an hour at room temperature in the high divalent salt condition (TKMC). Then excess media was removed, and a second coverslip was placed over the sample (the thickness of the Petri dish acting as the spacer). Nuclei were examined between cross-polarizers on a Leica inverted optical microscope with 100 oil objective 1.4 NA and a 1.4 NA oil condenser and recorded by using a Hitachi charge-coupled device camera.

***In Vivo* Pressure Assay.** Trypsinyzed cells were resuspended in PBS at a concentration of 3 10^6/ml. An aliquot (5 μl) cell suspension was diluted in 500 μl of H_2O, and 700 kPa of pressure was applied to the diluted cells for 90 sec. Cells were then seeded onto D-PolyLysine-coated coverslips (BD Biosciences), and after 30 min, were fixed in 4% buffered paraformaldehyde in PBS for 15 min at room temperature. Cells were washed three times with PBS and immunolabeled by using specific antibodies against lamin A/C (Santa Cruz Biotechnology; N-18), lamin B (Santa Cruz Biotechnology; M-20), and trimethyl-histone H3 (Lys-4) (Upstate Biotechnology, Lake Placid, NY) without detergent permeabilization. For controls, cells were permeabilized before fixation with either 40 μg/ml digitonin or 0.1% Nonidet P-40 as described in ref. 33. Exposure to pressure did affect cell viability, and not all cells attached to the glass slide. However, similar fractions of unattached cells (≈10%) were observed in WT and HGPS, thus cell mortality did not differentially affect the two cell lines. Coverslips were mounted by using Vectashield containing 10 μg/ml DAPI and observed on a Nikon E800 microscope by using 63 and 20 objectives. Approximately 300 cells were analyzed for each cell line, and the percentage of cells with antibody staining signal was scored.

We thank J. Broers, J. Ellenberg, and C. Stewart (National Cancer Institute, Frederick, MD) for reagents; D. Robinson for advice and access to equipment; and T. Karpova for technical support. Imaging was done at the National Cancer Institute Imaging Facility and the Johns Hopkins Microscope Facility. This research was supported by the Intramural Research Program of the National Institutes of Health, National Cancer Institute, and the Center for Cancer Research (to T.M.); National Research Service Award Fellowship 1 F32 GM074502 (to K.N.D.); and National Institutes of Health Grant R01GM48646 (to K.L.W.). T.M. and K.L.W. are Fellows of the Keith R. Porter Endowment for Cell Biology.

1. DeBusk, F. L. (1972) *J. Pediatr.* **80,** 697–724.
2. Uitto, J. (2002) *Trends. Mol. Med.* **8,** 155–157.
3. De Sandre-Giovannoli, A., Bernard, R., Cau, P., Navarro, C., Amiel, J., Boccaccio, I., Lyonnet, S., Stewart, C. L., Munnich, A., Le Merrer, M. & Levy, N. (2003) *Science* **300,** 2055.
4. Eriksson, M., Brown, W. T., Gordon, L. B., Glynn, M. W., Singer, J., Scott, L., Erdos, M. R., Robbins, C. M., Moses, T. Y., Berglund, P., *et al.* (2003) *Nature* **423,** 293–298.
5. Hutchison, C. J. (2002) *Nat. Rev. Mol. Cell Biol.* **3,** 848–858.
6. Goldman, R. D., Gruenbaum, Y., Moir, R. D., Shumaker, D. K. & Spann, T. P. (2002) *Genes Dev.* **16,** 533–547.
7. Glynn, M. W. & Glover, T. W. (2005) *Hum. Mol. Genet.* **14,** 2959–2969.
8. Goldman, R. D., Shumaker, D. K., Erdos, M. R., Eriksson, M., Goldman, A. E., Gordon, L. B., Gruenbaum, Y., Khuon, S., Mendez, M., Varga, R. & Collins, F. S. (2004) *Proc. Natl. Acad. Sci. USA* **101,** 8963–8968.
9. Scaffidi, P. & Misteli, T. (2005) *Nat. Med.* **11,** 440–445.
10. Liu, B., Wang, J., Chan, K. M., Tjia, W. M., Deng, W., Guan, X., Huang, J. D., Li, K. M., Chau, P. Y., Chen, D. J., *et al.* (2005) *Nat. Med.* **11,** 780–785.
11. Newport, J. W., Wilson, K. L. & Dunphy, W. G. (1990) *J. Cell Biol.* **111,** 2247–2259.
12. Lammerding, J., Schulze, P. C., Takahashi, T., Kozlov, S., Sullivan, T., Kamm, R. D., Stewart, C. L. & Lee, R. T. (2004) *J. Clin. Invest.* **113,** 370–378.
13. Panorchan, P., Schafer, B. W., Wirtz, D. & Tseng, Y. (2004) *J. Biol. Chem.* **279,** 43462–43467.
14. Dahl, K. N., Kahn, S. M., Wilson, K. L. & Discher, D. E. (2004) *J. Cell Sci.* **117,** 4779–4786.
15. Gruenbaum, Y., Margalit, A., Goldman, R. D., Shumaker, D. K. & Wilson, K. L. (2005) *Nat. Rev. Mol. Cell Biol.* **6,** 21–31.
16. Burke, B. & Stewart, C. L. (2002) *Nat. Rev. Mol. Cell Biol.* **3,** 575–585.
17. Wilson, K. L. (2005) *Proc. Natl. Acad. Sci. USA* **102,** 18767–18768.
18. Dahl, K. N., Engler, A. J., Pajerowski, J. D. & Discher, D. E. (2005) *Biophys. J.* **89,** 2855–2864.
19. Theret, D. P., Levesque, M. J., Sato, M., Nerem, R. M. & Wheeler, L. T. (1988) *J. Biomech. Eng.* **110,** 190–199.
20. Born, M. & Wolf, E. (1999) *Principles of Optics: Electromagnetic Theory of Propagation, Interference, and Diffraction of Light* (Cambridge Univ. Press, Cambridge, U.K.).
21. Gieffers, C. & Krohne, G. (1991) *Eur. J. Cell Biol.* **55,** 191–199.
22. Chaikin, P. M. & Lubensky, T. C. (1995) *Principles of Condensed Matter Physics* (Cambridge Univ. Press, Cambridge, U.K.).
23. Liu, J., Rolef Ben-Shahar, T., Riemer, D., Treinin, M., Spann, P., Weber, K., Fire, A. & Gruenbaum, Y. (2000) *Mol. Biol. Cell* **11,** 3937–3947.
24. Hutchison, C. J., Alvarez-Reyes, M. & Vaughan, O. A. (2001) *J. Cell Sci.* **114,** 9–19.
25. Markiewicz, E., Venables, R., Mauricio Alvarez, R., Quinlan, R., Dorobek, M., Hausmanowa-Petrucewicz, I. & Hutchison, C. (2002) *J. Struct. Biol.* **140,** 241–253.
26. Varga, R., Eriksson, M., Erdos, M. R., Olive, M., Harten, I., Kolodgie, F., Capell, B. C., Cheng, J., Faddah, D., Perkins, S., *et al.* (2006) *Proc. Natl. Acad. Sci. USA* **103,** 3250–3255.
27. Davies, P. F., Zilberberg, J. & Helmke, B. P. (2003) *Circ. Res.* **92,** 359–370.
28. Worman, H. J. & Gundersen, G. G. (2006) *Trends Cell Biol.* **16,** 67–69.
29. Lammerding, J., Hsiao, J., Schulze, P. C., Kozlov, S., Stewart, C. L. & Lee, R. T. (2005) *J. Cell Biol.* **170,** 781–791.
30. Broers, J. L., Machiels, B. M., van Eys, G. J., Kuijpers, H. J., Manders, E. M., van Driel, R. & Ramaekers, F. C. (1999) *J. Cell Sci.* **112,** 3463–3475.
31. Daigle, N., Beaudouin, J., Hartnell, L., Imreh, G., Hallberg, E., Lippincott-Schwartz, J. & Ellenberg, J. (2001) *J. Cell Biol.* **154,** 71–84.
32. Phair, R. D. & Misteli, T. (2000) *Nature* **404,** 604–609.
33. Adam, S. A., Marr, R. S. & Gerace, L. (1990) *J. Cell Biol.* **111,** 807–816.